

Electronic Supporting Information (ESI) for

Fluorescence sensor for Zn (II) based on Schiff base modified anthryl derivative with aggregation-induced emission enhancement and piezochromic characteristics

Mingdi Yang^{a, b}, Yan Zhang^a, Weiju Zhu^a, Huizhen Wang^a, Jing Huang^b, Longhuai Cheng^a,
Hongping Zhou^{a, *}, Jieying Wu^a, Yupeng Tian^a

^aKey Laboratory of Opto-Electronic Information Acquisition and Manipulation, Ministry of Education, College of Chemistry and Chemical Engineering, Anhui University, Hefei, 230601, P. R. China.

^bSchool of Materials and Chemical Engineering, Anhui Jianzhu University, Hefei, 230601, P. R. China.

**Corresponding author. Fax: +86-551-3861279; Tel: +86-551-3861279*

E-mail address: zhpzhp@263.net.

Contents

1. Spectroscopic properties of compounds **1-3**.
2. Selected dihedral angles and interaction patterns in the crystals of **1-3**.
3. UV-Vis absorption and fluorescence spectra of compounds **1-3** in six organic solvents.
4. PL spectra of compounds **1** and **3** in acetonitrile/methanol mixtures.
5. Response of compounds **1** and **3** to different metal ions in methanol/H₂O mixtures.
6. Calculation method of detection limit.
7. Calculation method of association constant.
4. Influence of pH and anions on the fluorescence spectra of **2**.
5. Reversibility and reversible cycles of **2**-Cu²⁺.
6. Competition experiments of **2**-Zn²⁺.
7. Influence of anions on the fluorescence spectra of **2**-Zn²⁺.
8. NMR and mass spectra for compounds **b, c** and **1-3**.
9. References.

Table S1. Spectroscopic properties of compounds **1–3**.

	solvents	λ_{\max}^a	ϵ_{\max}^b	λ_{\max}^c	$\Delta\nu^d$
1	Benzene	390	2.87	445	3155
	THF	390	3.07	440	3432
	Acetonitrile	387	3.16	436	3444
	DMF	391	3.06	441	3449
	Methanol	384	3.18	436	3220
	DMSO	390	2.36	445	3155
2	Benzene	407	5.69	509	2031
	THF	406	6.06	516	1904
	Acetonitrile	407	6.29	521	1860
	DMF	409	5.76	525	1851
	Methanol	424	6.88	519	2316
	DMSO	415	5.57	528	1939
3	Benzene	395	5.12	494	1971
	THF	398	6.56	510	1812
	Acetonitrile	396	5.32	524	1621
	DMF	399	4.96	530	1614
	Methanol	396	4.08	517	1692
	DMSO	402	5.04	533	1636

^a Absorption peak position in nm (1×10^{-5} mol L⁻¹). ^b Maximum molar absorbance in 10^4 mol⁻¹ L cm⁻¹. ^c Peak position of SPEF in nm (1×10^{-5} mol L⁻¹), excited at the absorption maximum. ^d Stokes shift in cm⁻¹.

Table S2. Selected dihedral angles and interaction patterns in the crystals of **1–3**.

		Dihedral angles (°)		Interactions	D (Å)
		Crystal state	Gas phase		
1	P ₁ -P ₂	1.79	11.53	C-H... π	2.703
	P ₂ -P ₃	65.29	52.93	C-H... π	3.486
				N...O	2.609
2	P ₁ -P ₂	35.58	9.12	C-H... π	3.170
	P ₂ -P ₃	66.71	48.17	C-H...O	2.675
				N...O	2.584
3	P ₁ -P ₂	44.83	41.70	C-H... π	2.977
	P ₂ -P ₃	79.63	51.18	C-H... π	2.974
				C-H... π	3.317

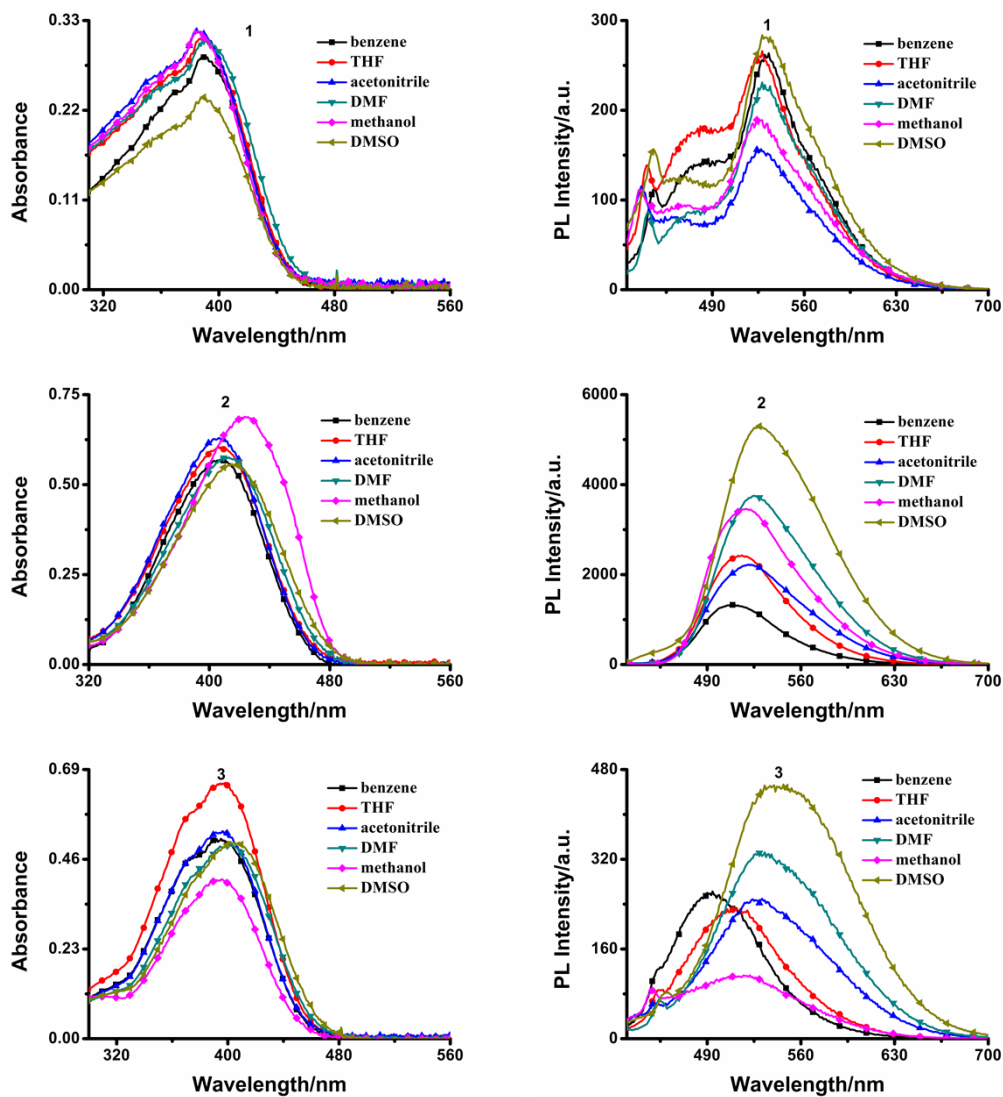


Fig. S1. One-photon absorption spectra and one-photon excitation fluorescence of compounds **1–3** in six organic solvents of different polarities with a concentration of $1 \times 10^{-5} \text{ mol L}^{-1}$.

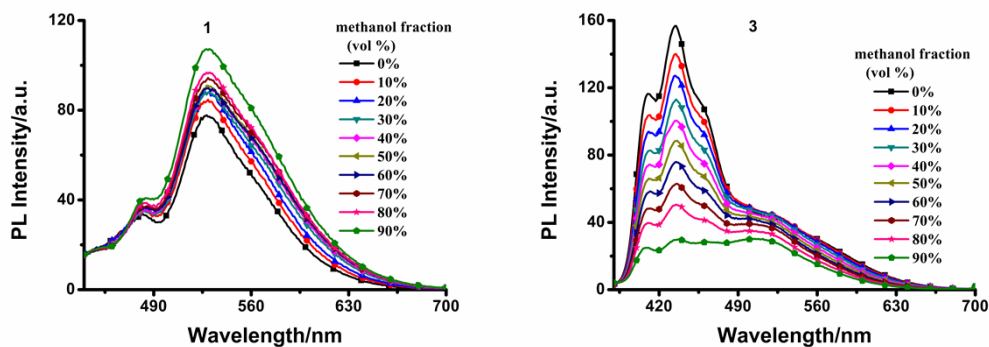


Fig. S2. PL spectra of compounds **1** and **3** in acetonitrile/methanol mixtures with different methanol fractions. The inset depicts the changes of PL peak intensity with different methanol fractions.

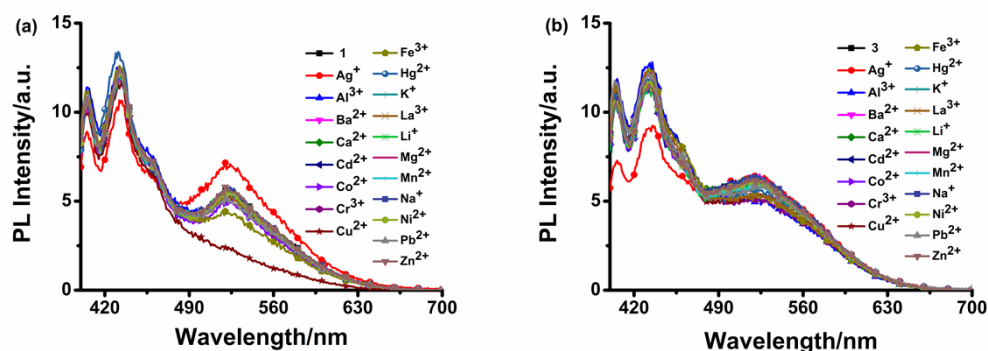


Fig. S3 Fluorescent spectra of **1** (a) and **3** (b) (10 μ M) in methanol/H₂O (4/1, v/v, pH 7.2) HEPES buffer solution with 1 equiv. different metal ions.

Calculation method of detection limit¹

The detection limit was calculated based on the UV-vis and fluorescence titration. To determine the S/N ratio, the absorbance or emission intensity of **2** without Cu²⁺ was measured by eight times and the standard deviation of blank measurements was determined. To gain the slop, the absorbance data at 432 nm or the fluorescent intensity data at 519 nm was plotted as a concentration of Cu²⁺. So the detection limit was calculated with the follow equation:

$$\text{Detection limit} = 3\sigma/K$$

Where σ is the standard deviation of blank measurements, and K is the slop between the absorbance or fluorescence versus Cu²⁺ concentration.

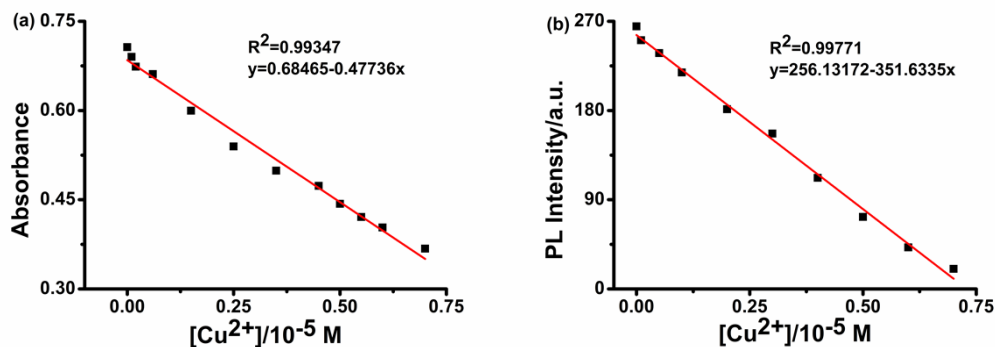


Fig. S4 Normalized response of absorption (a) and fluorescence (b) signal of **2** in the presence of different concentration Cu^{2+} .

Calculation method of association constant²

Assuming a 2:1 complex formation, the association constant was calculated on the basis of the titration curves of the sensor **2** with Cu^{2+} . Association constants were determined by a linear least square fitting of data with the following equation as a referenced method.

$$[\text{Cu}^{2+}] = 1/2K_a[2]_0 \cdot x / (1-x^2) + [2]_0/2 \cdot x$$

Where K_a is complex association constant; $[\text{Cu}^{2+}]$ is the concentration of Cu^{2+} ; $[2]_0$ is the initial concentration of sample; $x = (A - A_0) / (A_{\min} - A_0)$; A , A_0 and A_{\min} is the absorption intensity at 432 nm, free ligand and the absorption intensity at 432 nm upon the addition of Cu^{2+} .

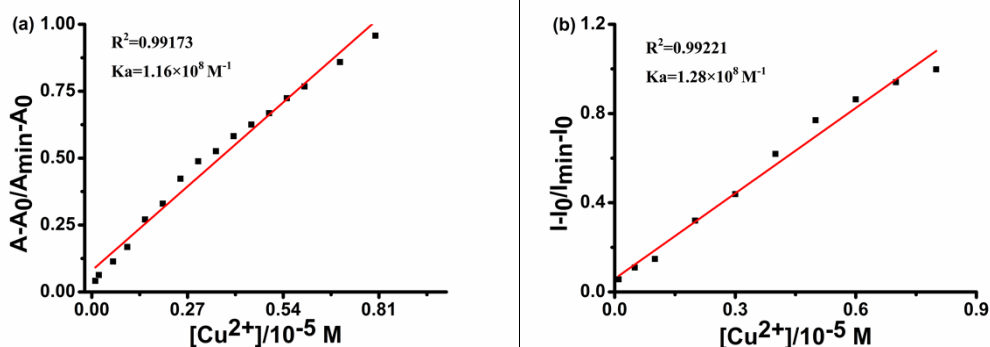


Fig. S5 Absorbance and fluorescence intensity ratio ($A-A_0/A_{\min}-A_0$ and $I-I_0/I_{\min}-I_0$) as the square of Cu^{2+} concentration.

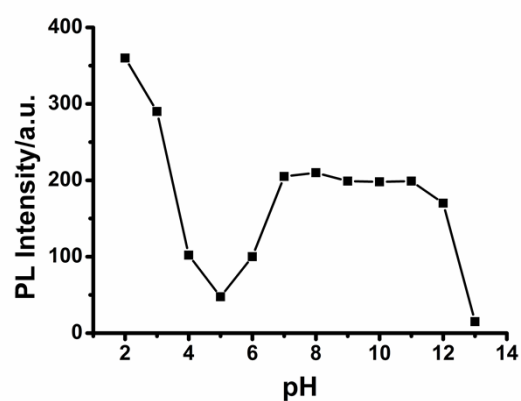


Fig. S6 Influence of pH on the fluorescence spectra of **2** (fluorescence intensity at 519 nm).

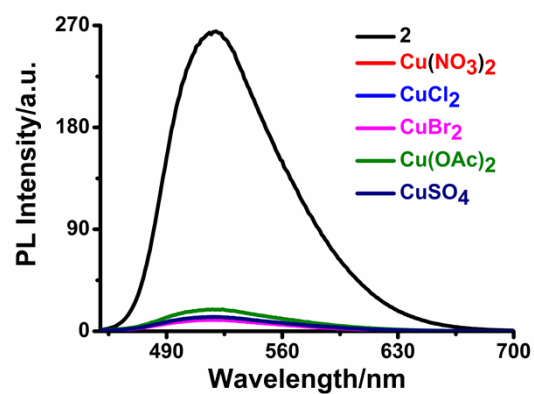


Fig. S7 Fluorescence spectra of **2** with addition of Cu^{2+} with different counter anions in methanol/ H_2O (4/1, v/v, pH 7.2) HEPES buffer solution.

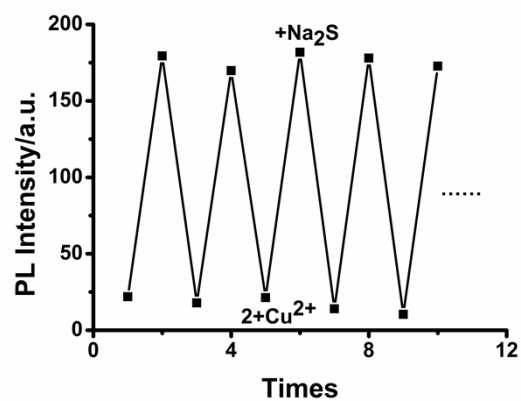


Fig. S8 Sensor reversibility and reversible cycles of $\text{2}+\text{Cu}^{2+}$.

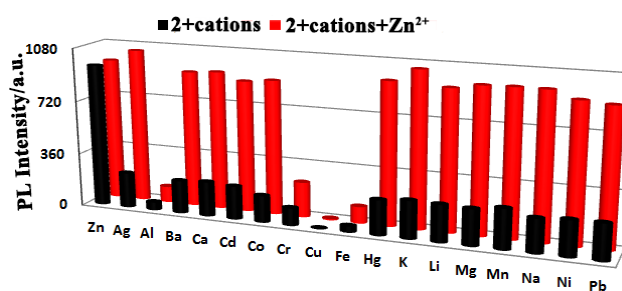


Fig. S9 Fluorescence intensity change of **2** (10 μ M) upon addition of various metal ions (10 μ M) in and without the presence of Zn²⁺ (10 μ M) in methanol solution.

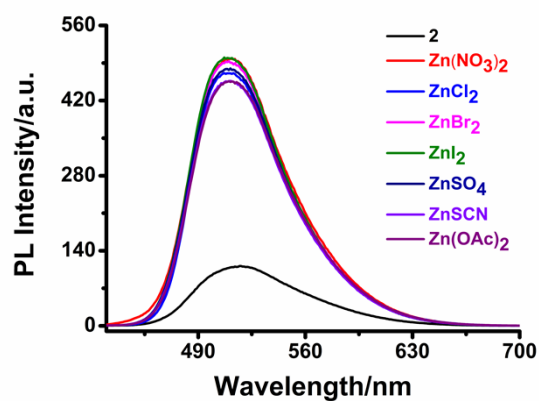


Fig. S10 Fluorescence spectra of **2** with addition of Zn²⁺ with different counter anions in methanol solution.

Fig. S11. ^1H NMR spectrum of **b**.

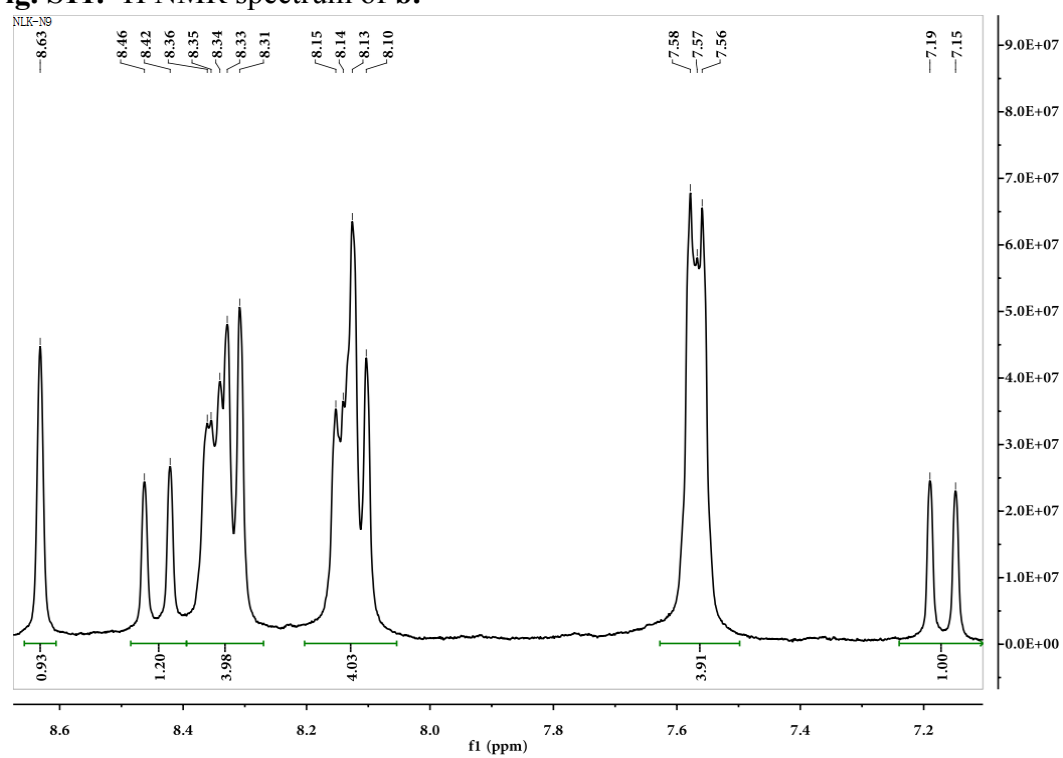


Fig. S12. ^{13}C NMR spectrum of **b**.

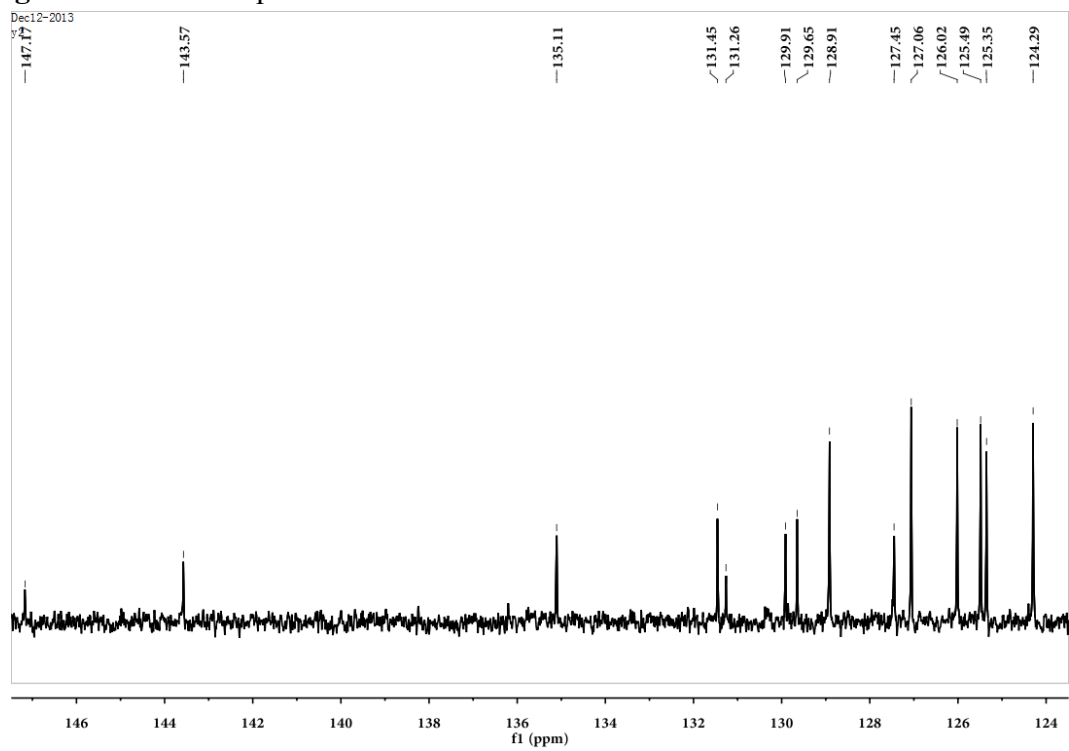


Fig. S13. ^1H NMR spectrum of **c**.

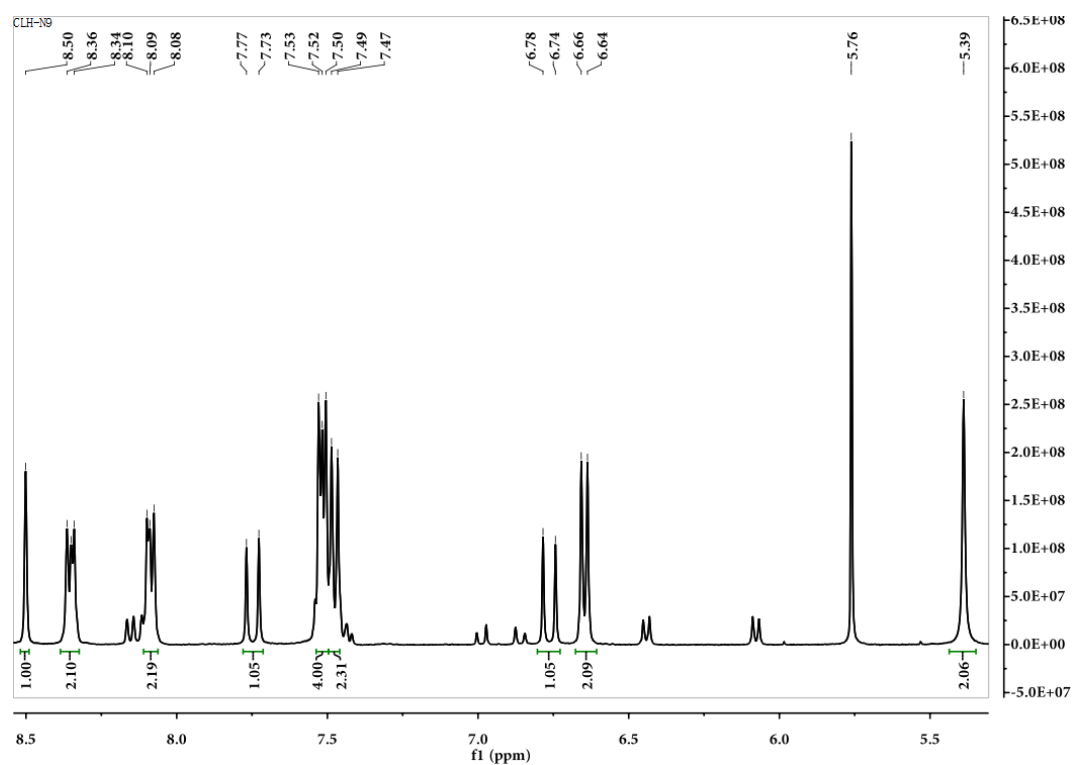


Fig. S14. ^{13}C NMR spectrum of **c**.

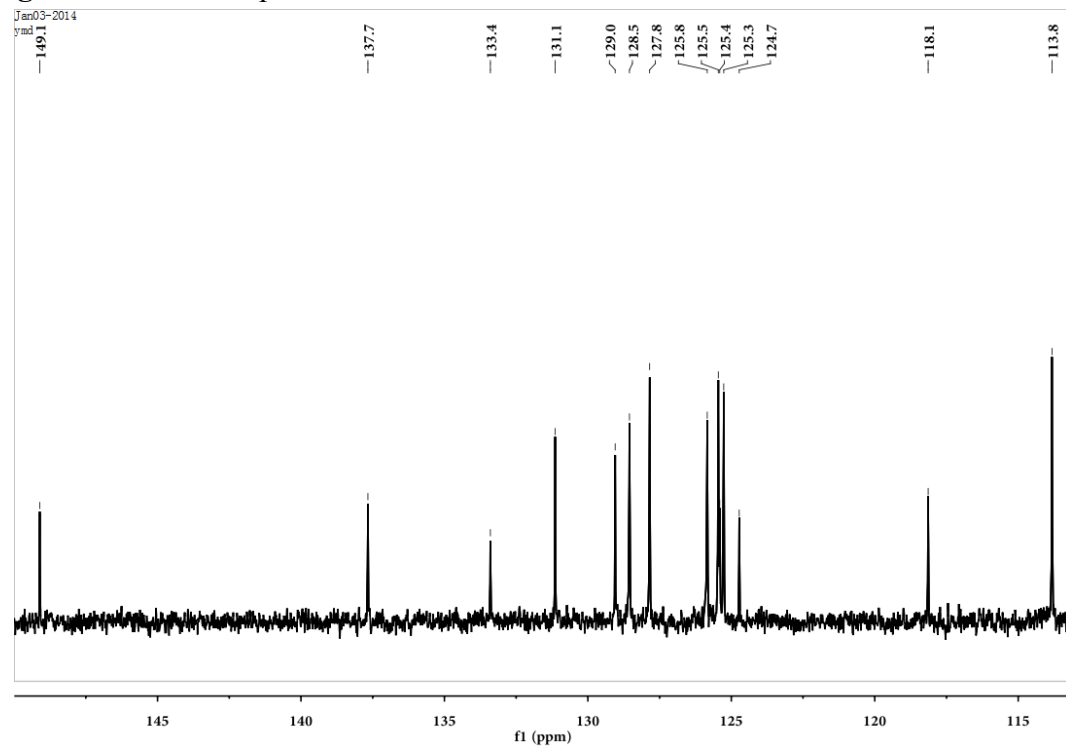


Fig. S15. ^1H NMR spectrum of **1**.

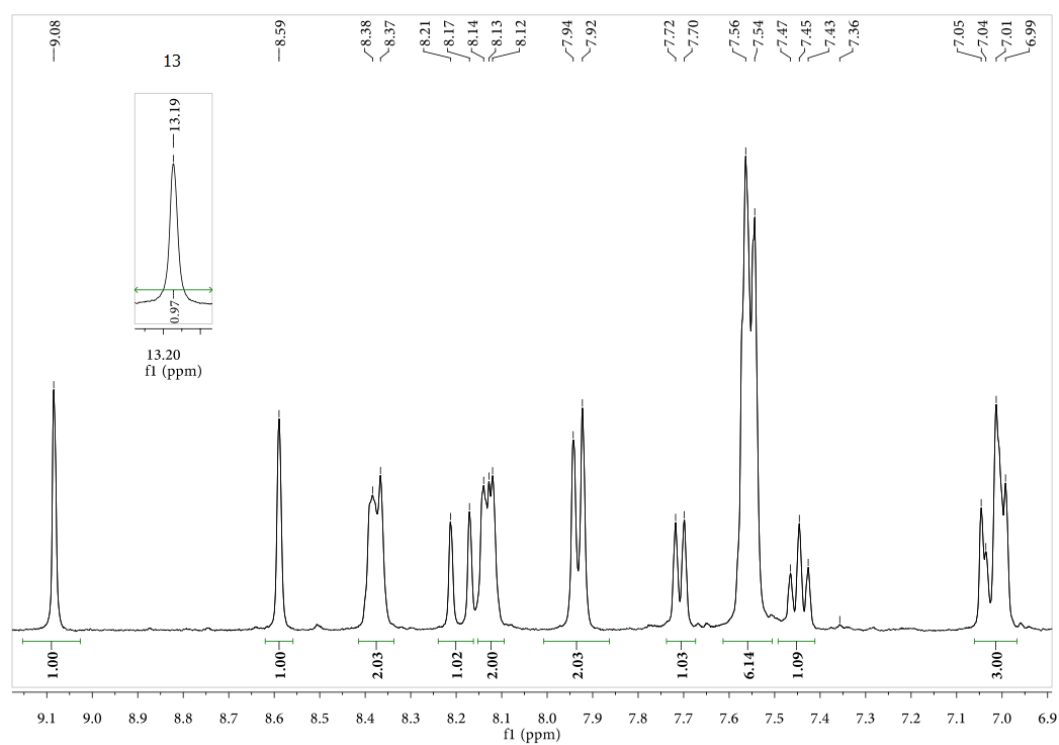


Fig. S16. ^{13}C NMR spectrum of **1**.

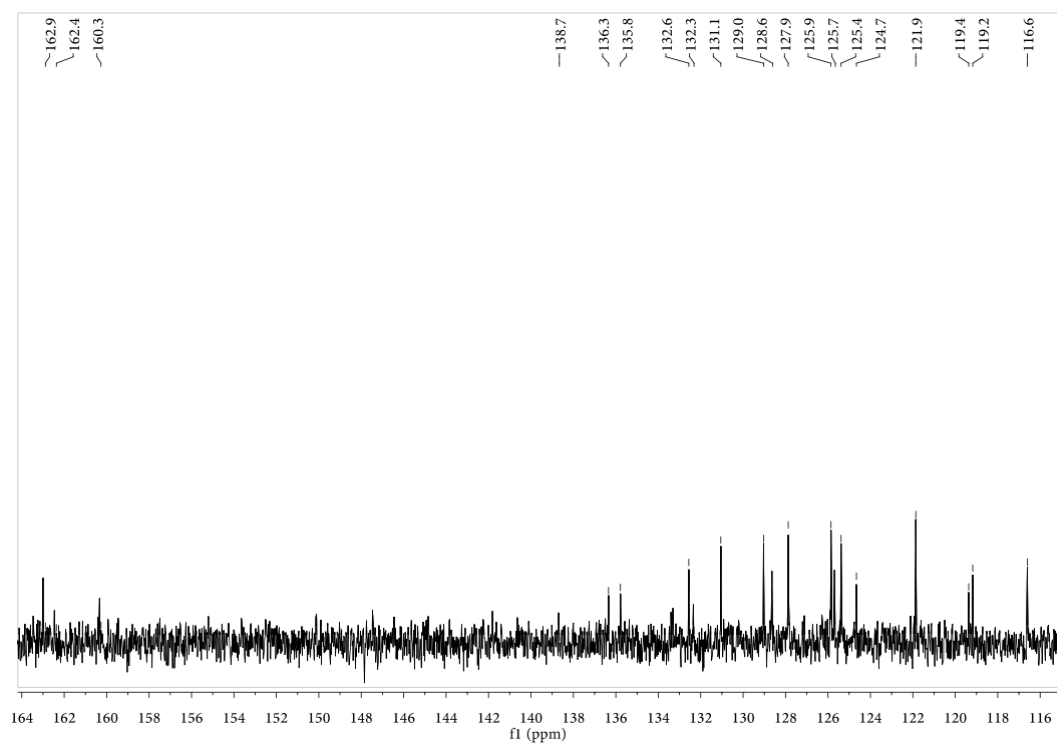


Fig. S17. MS spectrum of **1**.

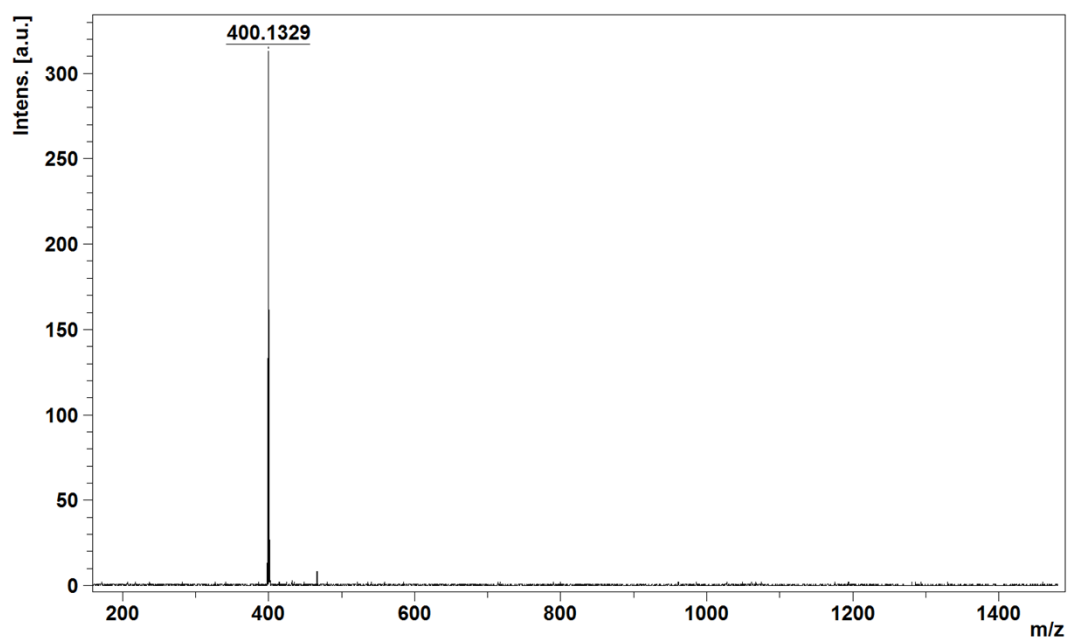


Fig. S18. ^1H NMR spectrum of **2**.

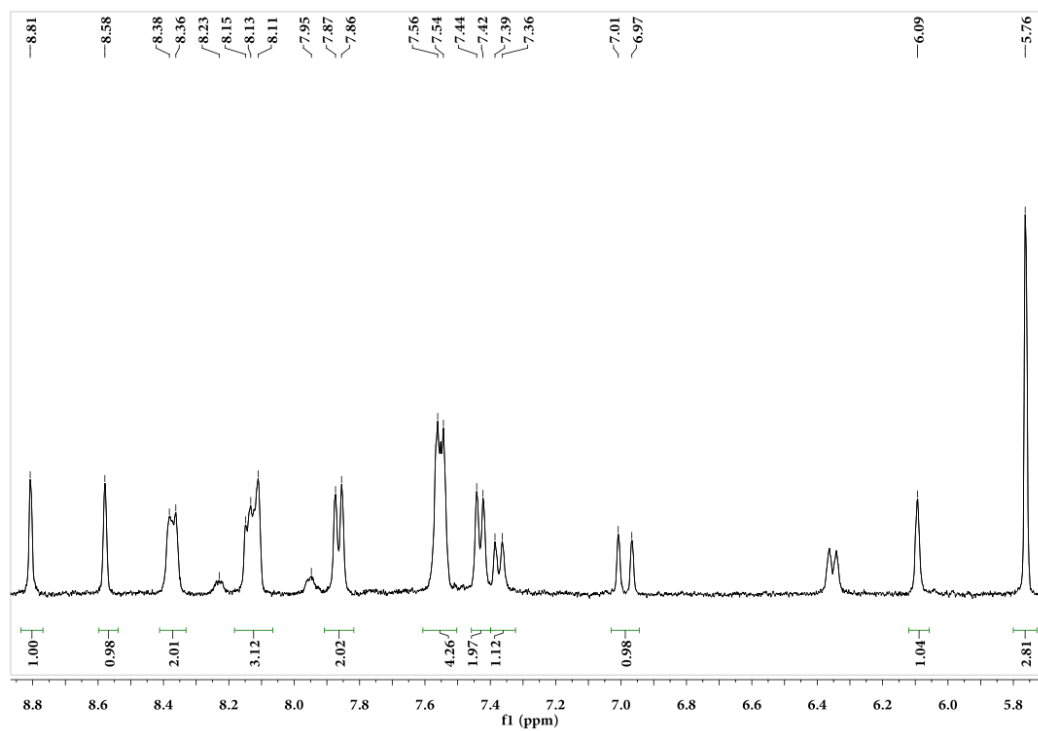


Fig. S19. ^{13}C NMR spectrum of **2**.

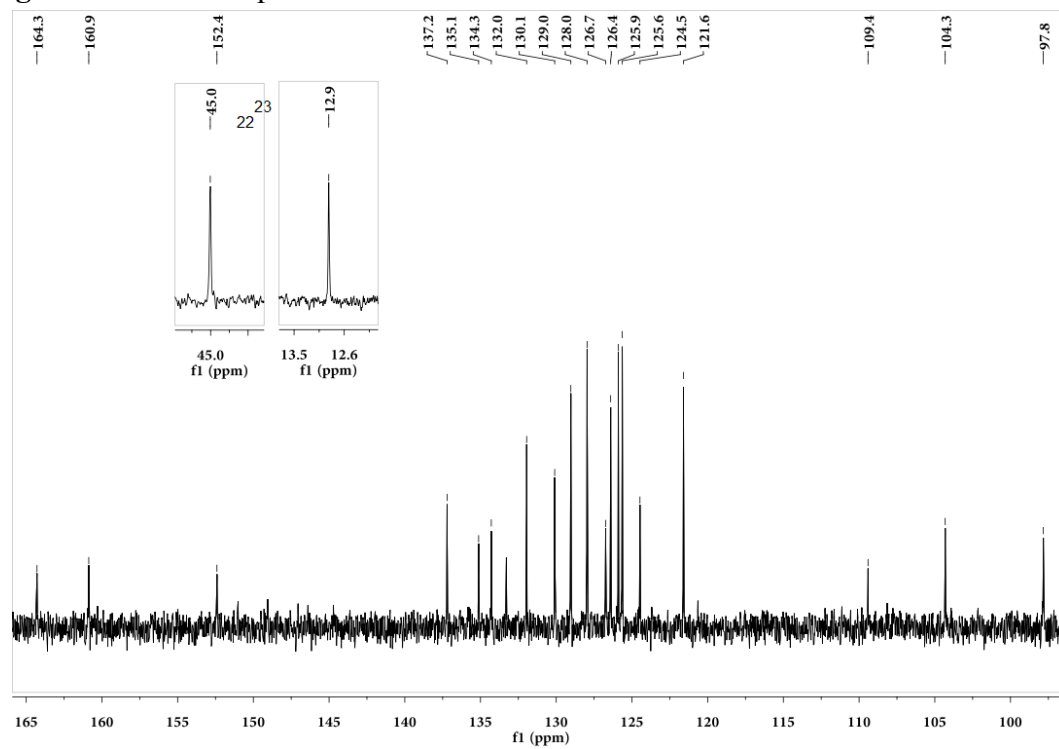


Fig. S20. MS spectrum of **2**.

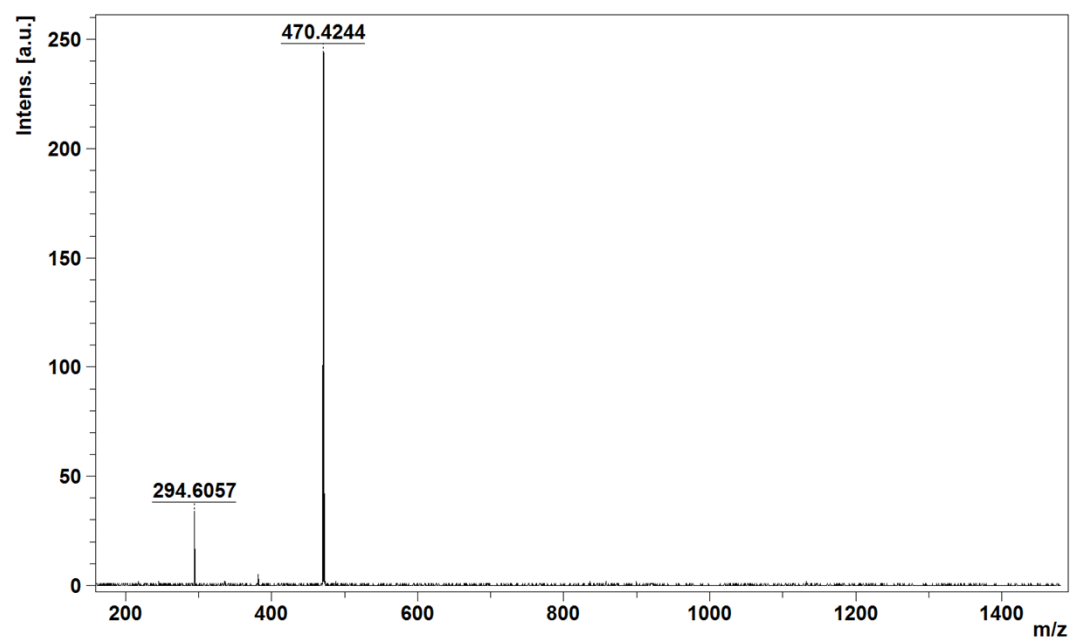


Fig. S21. ^1H NMR spectrum of **3**.

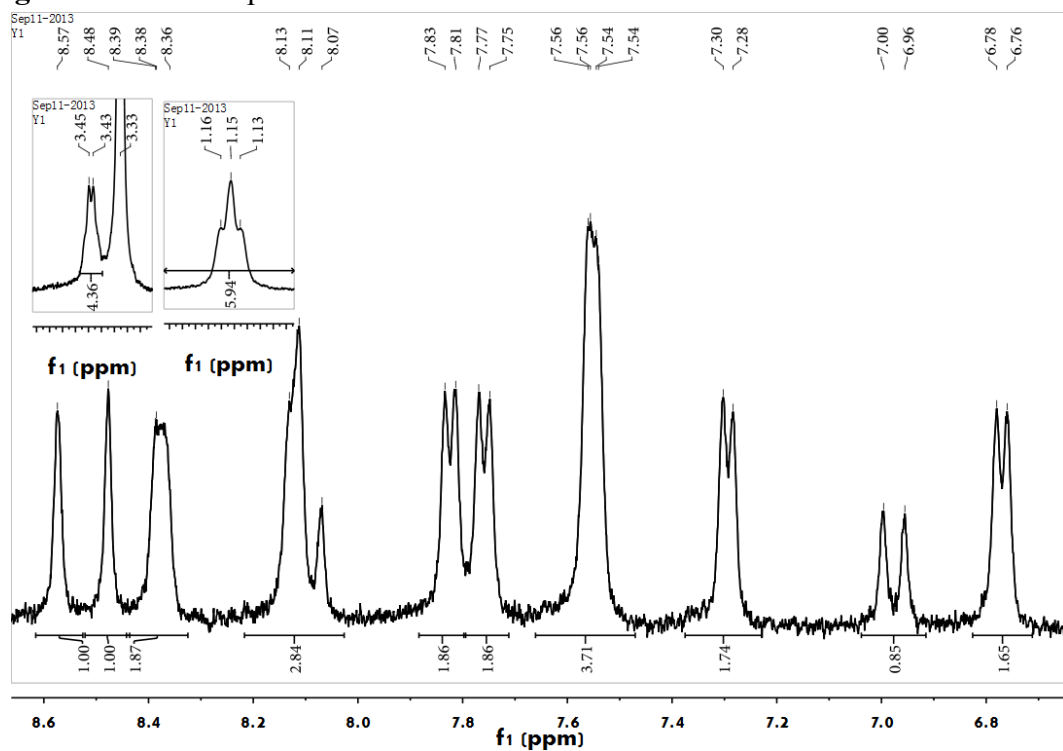


Fig. S22. ^{13}C NMR spectrum of **3**.

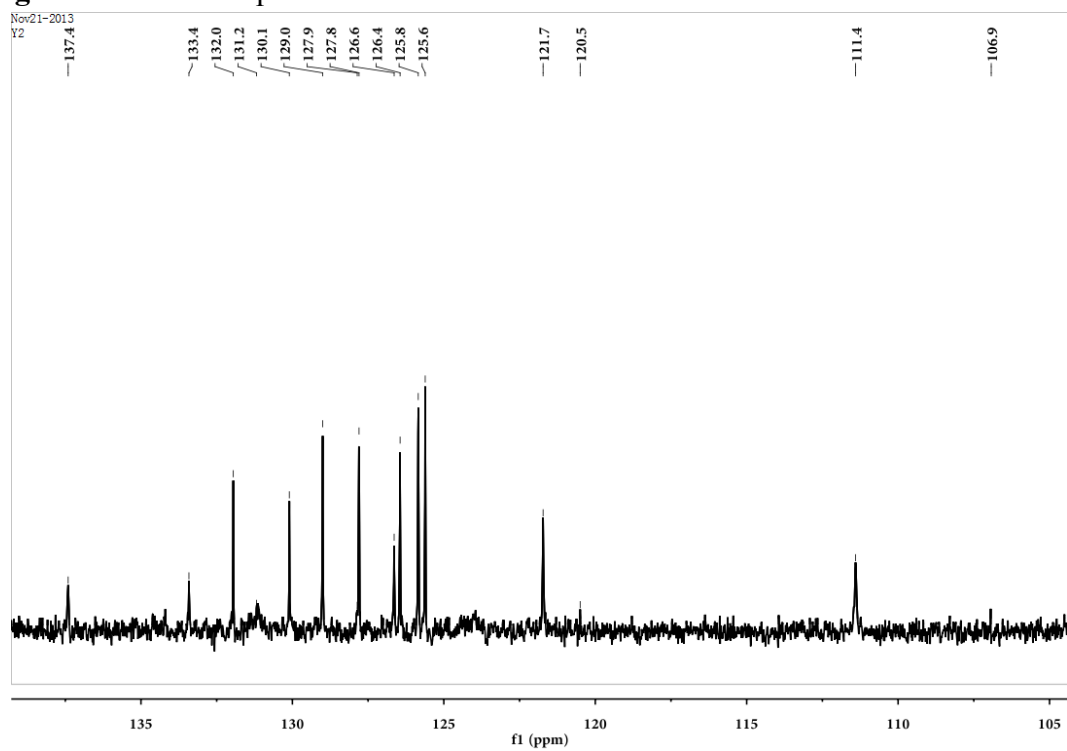
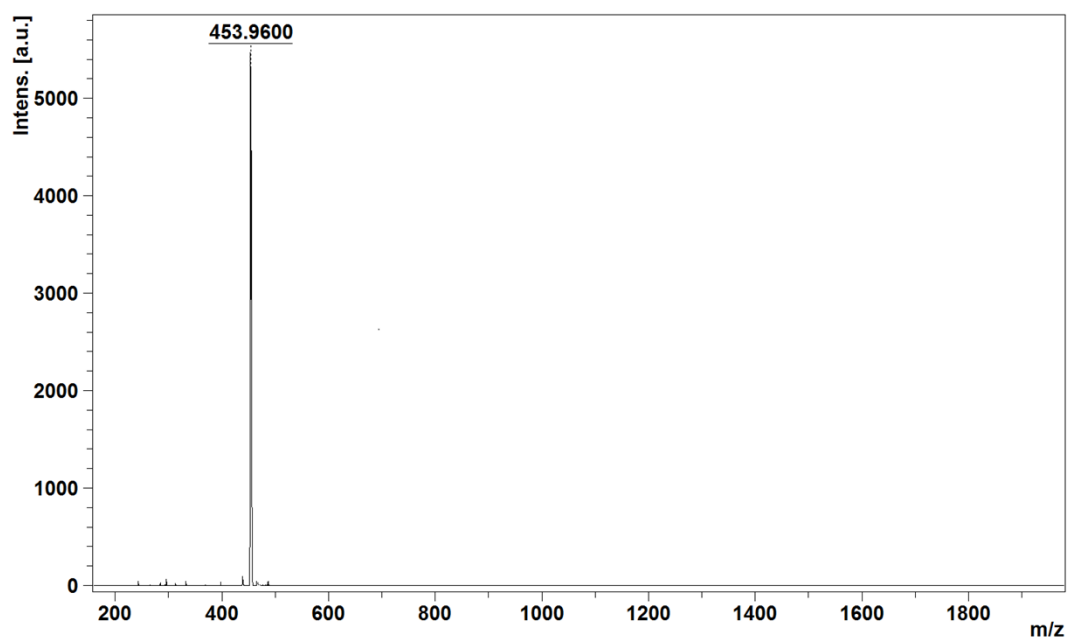


Fig. S23. MS spectrum of **3**.



Reference

1. J. S. Wu, W. M. Liu, X. Q. Zhuang, P. F. Wang, *Org. Lett.* 2007, **9**, 33.
2. M. Shellaiah, Y. H. Wu, A. Singh, M. V. R. Raju, H. C. Lin, *J. Mater. Chem. A* 2013, **1**, 1310.